JOURNAL OF SOLID STATE CHEMISTRY 53, 217–226 (1984)

The Phase Relations in the In_2O_3–A_2O_3–BO Systems at Elevated Temperatures [*A*: Fe or Ga, *B*: Cu or Co]

NOBORU KIMIZUKA* AND EIJI TAKAYAMA

National Institute for Research in Inorganic Materials
1-1, Namiki, Sakuramura, Niiharigun, Ibaraki-ken, Japan 305

Received September 14, 1983; in revised form January 20, 1984

The phase relations in the In_2O_3–Fe_2O_3–CuO system at 1000°C, the In_2O_3–Ga_2O_3–CuO system at 1000°C, the In_2O_3–Fe_2O_3–CoO system at 1300°C, and the In_2O_3–Ga_2O_3–CoO system at 1300°C were determined by means of a classical quenching method. $InFeCuO_4$ (a = 3.3743(4) Å, c = 24.841(5) Å), $InGaCuO_4$ (a = 3.3497(2) Å, c = 24.822(3) Å), and $InGaCoO_4$ (a = 3.3091(2) Å, c = 25.859(4) Å) having the $YbFe_2O_4$ crystal structure, $In_2Fe_2CuO_7$ (a = 3.3515(2) Å, c = 28.871(3) Å), $In_2Ga_2CuO_7$ (a = 3.3319(1) Å, c = 28.697(2) Å), and $In_2FeGaCuO_7$ (a = 3.3421(2) Å, c = 28.817(3) Å) having the $Yb_2Fe_3O_7$ crystal structure, and $In_3Fe_3CuO_{10}$ (a = 3.3432(3) Å, c = 61.806(6) Å) having the $Yb_3Fe_4O_{10}$ crystal structure were found as the stable ternary phases. There is a continuous series of solid solutions between $InFeCoO_4$ and Fe_2CoO_4 which have the spinel structure at 1300°C. The crystal chemical roles of Fe^{3+} and Ga^{3+} in the present ternary systems were qualitatively compared.

Introduction

Recently we have established the phase diagrams of the Ln_2O_3–FeO–Fe_2O_3 systems (*Ln*: lanthanide elements and Y) at elevated temperatures under controlled oxygen partial pressures and reported a series of new homologous compounds $(LnFeO_3)_nFeO$ (n = 1, 2, 3 . . .) with layered structures (*1*). The single crystal structural analyses for $YbFe_2O_4$ and $Yb_2Fe_3O_7$ were performed by Kato *et al.* (*2, 3*). $Yb_3Fe_4O_{10}$, $Yb_4Fe_5O_{13}$, and the higher order compounds were analyzed by means of both electron diffraction and powder X-ray diffraction methods (*4, 5*). The crystal structural models for $YbFe_2O_4$ and $Yb_2Fe_3O_7$ are shown in Figs. 1 and 2, respectively.

Tanaka *et al.* (*6*) measured the electrical conductivities, specific heat, and Mössbauer spectra of YFe_2O_{4+x} (x = −0.05 ~ 0.00) and observed the conductivity gap (about 10^5 ohm^{-1} cm^{-1}) and specific heat anomaly at about 250 K. Nakagawa *et al.* (*7*) also found crystallographic transformations in YFe_2O_{4+x} at the lower temperatures. Tanaka *et al.* (*6*) concluded that the transition in $YFe_2O_{4.00}$ belongs to the Verway type observed in Fe_3O_4 (*8*) and Ti_4O_7 (*9*). Both the Fe^{2+} and the Fe^{3+} occupy the same crystallographic site formed by a trigonal bipyramid of the oxygen ions; however, the nonstoichiometry in YFe_2O_{4+x} causes the complicated properties observed in the electrical transport phenomena, the magnetic behavior and the Mössbauer spectra. The details in the mechanism of the transitions are still open to question.

---

* To whom all correspondence should be addressed.

0022-4596/84 $3.00

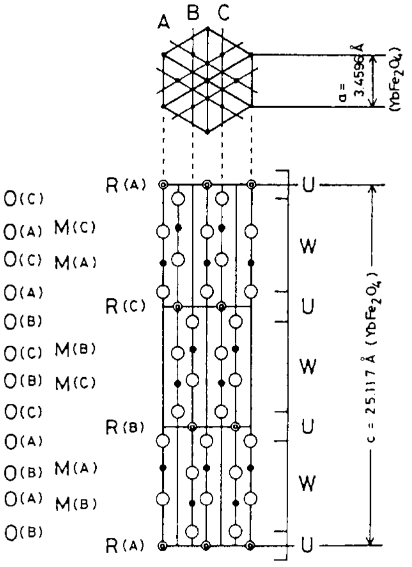

FIG. 1. The crystal structure of $YbFe_2O_4$ (space group: $R\bar{3}m$). (R) Yb ion, (M) Fe ion, (O) O ion, (U) Yb_2O_3 layer, (W) Fe_4O_5 layer. A, B, and C indicate the positions of the ions.

In order to stop the electron transfer between Fe^{2+} and Fe^{3+} in the $LnFe_2O_4$ compounds (*Ln*: Er, Ho, Tm, Yb, Lu, and Y), we replaced the Fe^{2+} ion with another divalent cation such as Cu^{2+}, Zn^{2+}, Mg^{2+}, Co^{2+}, or Mn^{2+}. The compounds obtained were $LnFeCuO_4$, $LnFeCoO_4$ (*Ln*: Lu, Yb, or Tm), $LnFeMnO_4$ (*Ln*: Lu, Yb, Tm, Ho, or Y), and $LnFeMgO_4$ (*Ln*: Lu, Yb, Tm, or Ho) which are isostructural with $YbFe_2O_4$ (*11*). The phase relations in the Yb_2O_3–Fe_2O_3–CuO system at 1000°C, the Yb_2O_3–Ga_2O_3–CuO system at 1000°C, the Yb_2O_3–Fe_2O_3–CoO System at 1300 and 1200°C, the Yb_2O_3–Fe_2O_3–ZnO system at 1300°C, and the Yb_2O_3–Ga_2O_3–ZnO system at 1350 and 1200°C were also determined by a classical quenching method (*10*) and the thermochemical stability conditions of each *Ln* $FeMO_4$ and $LnGaMO_4$ phase were reported by Kimizuka and Takayama (*11*). Each *Ln* $FeMO_4$ and $LnGaMO_4$ phase is stable above a certain temperature and decomposes to $LnFeO_3$ and *M*O phases or $Ln_3Ga_5O_{12}$, Ln_2O_3, and *M*O phases below that temperature, respectively.

In the $Ln_2Fe_3O_7$ compounds (*Ln*: Lu, Yb, or Tm), there are Fe_2O_3 and Fe_4O_5 layers which are separated by a Ln_2O_3 layer (*3*). The Mössbauer study and neutron diffraction analysis for $Lu_2Fe_3O_7$ and $Yb_2Fe_3O_7$ indicate that there may be an interaction of spins in the Fe_2O_3 and Fe_4O_5 layers (*12*). To study that interactions in more simple cases, we tried to replace the Fe^{2+} ion in $Yb_2Fe_3O_7$ with another divalent cation such as Cu^{2+} to stop the electron transfer in the Fe_4O_5 layer. In the present paper, we report the phase relations in the In_2O_3–Fe_2O_3–CuO system at 1000°C, the In_2O_3–Ga_2O_3–CuO system at 1000°C, the In_2O_3–Fe_2O_3–CoO system at 1300°C, and the In_2O_3–Ga_2O_3–CoO system at 1300°C which were determined by means of a classical quenching method. In these systems $(InFeO_3)_nCuO$ (n = 1, 2, and 3), $(InGaO_3)_nCuO$ (n = 1 and 2), $(InGaO_3)_nCoO$ (n = 1) which are isostructural with $(YbFeO_3)_nFeO$ (n = 1, 2, and 3)

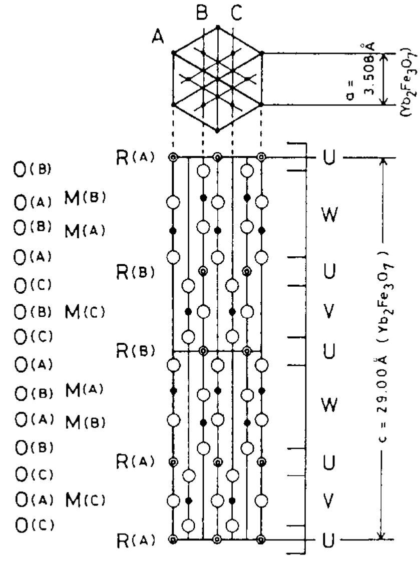

FIG. 2. The crystal structure of $Yb_2Fe_3O_7$ (space group: $P6_3/mmc$). (R) Yb ion, (M) Fe ion, (O) O ion. (U) Yb_2O_3 layer, (V) Fe_2O_3 layer, (W) Fe_4O_5 layer. A, B, and C indicate the positions of the ions.

and $InFeCoO_4$ with the spinel structure were obtained as the ternary stable phases.

Experimental

The experimental methods and apparatus used in the present study have been described in Refs. (*10, 11*). In_2O_3 (99.99%) was used as a starting compound. Prior to mixing, we heated it at 800°C in air for 1 day. Other starting compounds are the same as in Refs. (*10, 11*). Calculated amounts of each end member: In_2O_3, A_2O_3 (A: Fe or Ga), BO(B: Cu or Co) was weighed to the nearest milligram. Each batch was thoroughly mixed under ethyl alcohol in an agate mortar and sealed in a Pt tube, and fired at successively higher temperatures until equilibrium was obtained. After each heat treatment, the specimen was rapidly cooled in water. Equilibrium was considered to be attained when the X-ray powder diffraction pattern of a specimen showed no change with successive heat treatment of the specimen. Identification of phases and determination of lattice constants were performed by means of powder X-ray method on a scintillation counter diffractometer, using silicon as a standard material. Mn-filtered Fe$K\alpha$ radiation was used for identification of all specimens and for measurement of d-values of compounds which contained iron. Measurement of d-values of other compounds was done using Ni-filtered Cu$K\alpha$ radiation. Lattice constants were calculated by means of least squares.

Results and Discussion

[I] *The Phase Relations in the* In_2O_3–Fe_2O_3–CuO *System at* 1000°C

In_2O_3 ("C" type rare earth sesquioxide structure, a = 10.118(Å) (*13*)), Fe_2O_3 (α-form, corundum) (*14*), and CuO (PtS structure) (*15*) were stable. In the In_2O_3–CuO system, there was one stable phase of $In_2Cu_2O_5$ as previously reported (*15, 16*). In the CuO–Fe_2O_3 system, there was a stable phase of Fe_2CuO_4 with a spinel structure which had been reported in the Cu_2O–CuO–Fe_3O_4–Fe_2O_3 system at elevated temperatures under various oxygen partial pressures (*15, 17*). The solid solution range of Fe_2CuO_4 in Fig. 3 was cited from the Refs. (*15, 17*).

In the Fe_2O_3–In_2O_3 system, no binary compounds were detected during a heating period of 6 months.

A sample with $In_2O_3 : Fe_2O_3 : CuO$ = 0.15 : 0.75 : 0.10 (all ratios given in this paper are mole ratios) which was heated for 27 days was identified as a mixture of $In_2Fe_2CuO_7$, $In_3Fe_3CuO_{10}$, and "Fe_2O_3" phases, and a sample of $In_2O_3 : Fe_2O_3 : CuO$ = 0.20 : 0.70 : 0.10 was identified as a mixture of $In_3Fe_3CuO_{10}$, "In_2O_3," and "Fe_2O_3." The d-spacings of "Fe_2O_3" and "In_2O_3" showed these compounds to be solid solutions. After heating a mixture of $In_2O_3 : Fe_2O_3$ = 0.05 : 0.95 for 30 days, a single phase having a corundum structure was obtained.

Since solid state reactions among three components were faster than those between two components of In_2O_3 and Fe_2O_3

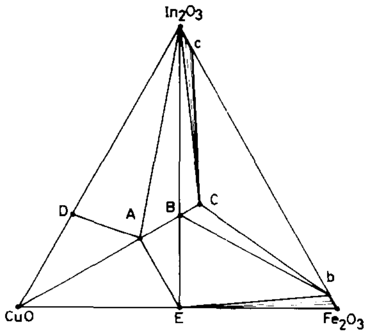

FIG. 3. The phase diagram of the In_2O_3–Fe_2O_3–CuO system at 1000°C. (A) $InFeCuO_4$, (B) $In_2Fe_2CuO_7$, (C) $In_3Fe_3CuO_{10}$, (D) $In_2Cu_2O_5$, (E) Fe_2CuO_4, (b) $In_2O_3 : Fe_2O_3$ = 0.05 : 0.95 (in moles), (c) $In_2O_3 : Fe_2O_3$ = 0.925 : 0.075 (in moles).

(*10*), we determined the solid solution ranges, not from experiments of a binary system but from those of a ternary one. We concluded that the solid solution range of "In_2O_3" extended to a composition of In_2O_3 : Fe_2O_3 = 0.925 : 0.075 and that of "Fe_2O_3" was to In_2O_3 : Fe_2O_3 = 0.05 : 0.95.

In the In_2O_3–Fe_2O_3–CuO system, there were three stable phases, namely, $InFeCuO_4$, $In_2Fe_2CuO_7$, and $In_3Fe_3CuO_{10}$.

$(InFeO_3)_nCuO$ (n = 1, 2, or 3) was isostructural with the corresponding compound $(YbFeO_3)_nFeO$ (n = 1, 2, or 3).

The above conclusions were obtained from the X-ray powder diffraction patterns shown in Table I. The corresponding lattice constants are shown in Table II. From these results we can conclude that the Cu^{2+} ion in $(InFeO_3)_nCuO$ (n = 1, 2, and 3) occupies the position of Fe^{2+} in $YbFe_2O_4$, $Yb_2Fe_3O_7$, and $Yb_3Fe_4O_{10}$, respectively.

We heated $In_3Fe_3CuO_{10}$ at 1100°C for 1 week; however, no decomposition was detected. A mixture of In_2O_3 : Fe_2O_3 : CuO = 0.40 : 0.40 : 0.20 was heated at 1100°C for 1 week; however, no $In_4Fe_4CuO_{13}$ was obtained, but "In_2O_3," "Fe_2O_3," and $In_3Fe_3CuO_{10}$ phases were observed. $(InFeO_3)_nCuO$ (n = 1, 2, and 3) were heated at 700°C for 21 days; but no decompositions were detected and X-ray diffraction peaks of each compound became sharper with increasing heating period. Schneider *et al.* (*18*) reported the phase diagrams of the In_2O_3–Fe_2O_3 system at elevated temperatures. They indicated that the "Fe_2O_3"

TABLE Ia

POWDER X-RAY DATA FOR $InFeCuO_4$, $InGaCuO_4$, AND $InGaCoO_4$

	$InFeCuO_4$			$InGaCuO_4$			$InGaCoO_4$		
h k l	d_0 (Å)	d_c (Å)	*I*(%)	d_0 (Å)	d_c (Å)	*I*(%)	d_0 (Å)	d_c (Å)	*I*(%)
0 0 3	8.297	8.280	21	8.276	8.274	12	8.622	8.620	15
0 0 6	4.143	4.140	33	4.137	4.137	29	4.311	4.310	23
1 0 1	2.903	2.902	100	2.881	2.881	100	2.847	2.848	95
1 0 $\bar{2}$	2.844	2.845	5	2.827	2.825	6	2.797	2.798	5
0 0 9	2.762	2.760	56	2.759	2.758	61	2.874	2.873	72
1 0 4	2.644	2.644	92	2.627	2.628	98	2.619	2.620	100
1 0 $\bar{5}$	2.519	2.519	85	2.504	2.505	88	2.506	2.507	73
1 0 7	2.256	2.256	10	2.246	2.245	5	2.265	2.264	5
1 0 $\bar{8}$	2.128	2.128	21	2.119	2.119	19	2.144	2.144	25
0 0 12	2.071	2.070	2	2.069	2.069	3	—	—	—
1 0 10	1.8928	1.8927	58	1.8868	1.8860	53	1.9202	1.9199	43
1 1 0	1.6863	1.6871	70	1.6746	1.6749	68	1.6546	1.6545	57
0 0 15	1.6549	1.6561	12	1.6551	1.6548	6	—	—	—
1 1 3		1.6532		1.6415	1.6416	3	—	—	—
1 0 13	1.5997	1.5993	11	1.5949	1.5949	14	1.6343	1.6341	23
1 1 6	1.5624	1.5624	13	1.5521	1.5525	10	—	—	—
1 0 $\overline{14}$	1.5168	1.5167	40	1.5124	1.5128	38	1.5524	1.5526	38
2 0 $\bar{1}$	1.4585	1.4586	15	1.4483	1.4480	10	—	—	—
1 1 9	1.4396	1.4395	50	1.4314	1.4316	41	1.4340	1.4338	60
2 0 $\bar{4}$	1.4219	1.4223	15	1.4126	1.4124	13	1.3993	1.3989	12
2 0 5	1.4015	1.4017	14	1.3925	1.3923	14	1.3807	1.3809	10
2 0 $\overline{10}$	—	—	—	1.2522	1.2523	11	1.2531	1.2533	9

Note. The *hkl* are given as a hexagonal crystal system.

TABLE Ib

POWDER X-RAY DATA FOR $In_2Ga_2CuO_7$, $In_2Fe_2CuO_7$, AND $In_2FeGaCuO_7$

	$In_2Ga_2CuO_7$			$In_2Fe_2CuO_7$			$In_2FeGaCuO_7$		
h k l	d_0 (Å)	d_c (Å)	*I*(%)	d_0 (Å)	d_c (Å)	*I*(%)	d_0 (Å)	d_c (Å)	*I*(%)
0 0 4	7.184	7.174	8	7.248	7.218	32	7.225	7.204	14
0 0 6	4.780	4.783	9	4.813	4.812	18	4.809	4.803	12
0 0 8	3.589	3.587	7	3.612	3.609	12	3.605	3.602	8
1 0 0	2.868	2.886	90	2.905	2.902	22	—	—	—
0 0 10		2.870		2.888	2.887	100	2.881	2.882	93
1 0 1		2.871			2.888			2.880	
1 0 2	2.828	2.829	37	2.847	2.846	30	2.839	2.838	30
1 0 3	2.762	2.763	3	2.782	2.779	2	2.772	2.771	4
1 0 4	2.676	2.677	26	2.693	2.693	24	2.686	2.686	25
1 0 5	2.577	2.578	100	2.593	2.593	96	2.587	2.586	100
1 0 6	2.470	2.471	18	2.486	2.485	13	2.479	2.479	13
1 0 7	2.361	2.360	2	2.375	2.374	2	—	—	—
1 0 9	2.139	2.140	19	2.152	2.152	24	2.148	2.147	20
1 0 10	2.035	2.035	8	2.047	2.047	9	2.042	2.042	11
1 0 11	1.9349	1.9352	15	1.9467	1.9467	21	1.9423	1.9423	16
1 0 12	1.8417	1.8413	12	1.8523	1.8523	13	1.8481	1.8481	12
1 0 13	1.7539	1.7533	2	1.7638	1.7638	3	—	—	—
1 0 14	—	—	—	1.6810	1.6811	6	—	—	—
1 1 0	1.6659	1.6660	48	1.6759	1.6757	45	1.6709	1.6710	52
1 1 4	—	—	—	1.6327	1.6323	5	—	—	—
1 0 15	1.5946	1.5945	20	1.6040	1.6041	23	1.6005	1.6006	27
0 0 18		1.5943			1.6040			1.6008	
1 1 6	1.5735	1.5733	2	1.5822	1.5825	5	—	—	—
1 0 16	1.5230	1.5233	9	1.5324	1.5325	9	1.5290	1.5292	10
1 1 8	1.5109	1.5110	2	1.5200	1.5199	6	1.5160	1.5159	4
1 0 17	1.4570	1.4570	4	—	—	—	—	—	—
1 1 10	1.4407	1.4408	35	1.4492	1.4493	39	1.4450	1.4457	50
2 0 1		1.4410			1.4494			1.4453	
2 0 4	1.4143	1.4145	3	—	—	—	—	—	—
2 0 5	1.3993	1.3992	13	1.4075	1.4075	16	1.4038	1.4036	14
1 0 19	—	—	—	1.3459	1.3462	3	—	—	—
2 0 6	1.3815	1.3813	2	—	—	—	—	—	—
2 0 9	1.3144	1.3145	3	1.3223	1.3222	4	—	—	—
2 0 11	1.2626	1.2626	3	1.2698	1.2700	5	—	—	—
1 0 21	1.2351	1.2350	3	—	—	—	—	—	—
2 0 12		1.2354		—	—	—	—	—	—

phase could reach a molar composition of $In_2O_3 : Fe_2O_3 = 0.4 : 0.6$ and "In_2O_3" phase could reach a composition of $In_2O_3 : Fe_2O_3 = 0.7 : 0.3$ above 1000°C. In the present work, the solid solution range of each compound was narrower of that presented by Schneider *et al.* The phase relations in the In_2O_3–Fe_2O_3–CuO system at 1000°C are shown in Fig. 3

[*II*] *The Phase Relations in the In_2O_3–Ga_2O_3–CuO System at* 1000°C

β-Ga_2O_3 was stable (*19*). There was one Ga_2CuO_4 phase with a spinel structure in the CuO–Ga_2O_3 system. The solid solution range of Ga_2CuO_4 was narrower than that of Fe_2CuO_4. The phase diagram of the Ga_2O_3–In_2O_3 system was first reported by

TABLE Ic

POWDER X-RAY DATA FOR $In_3Fe_3CuO_{10}$

$h\ k\ l$	d_0 (Å)	d_c (Å)	I (%)
0 0 3	20.72	20.60	13
0 0 6	10.37	10.30	9
0 0 9	6.887	6.867	24
0 0 12	5.155	5.150	14
0 0 15	4.124	4.120	6
0 0 18	3.435	3.434	4
0 0 21	2.943	2.943	62
1 0 1	2.892	2.892	100
1 0 4	2.845	2.846	40
$\bar{1}$ 0 5	2.820	2.819	21
1 0 7	2.752	2.751	6
$\bar{1}$ 0 8	2.712	2.711	11
1 0 10	2.621	2.622	78
$\bar{1}$ 0 11	2.574	2.574	62
$\bar{1}$ 0 14	2.421	2.421	4
1 0 19	2.162	2.163	21
$\bar{1}$ 0 20	2.113	2.113	25
1 0 22	2.016	2.016	17
1 0 25	1.8799	1.8801	18
$\bar{1}$ 0 29	1.7163	1.7164	7
1 1 0	1.6713	1.6716	81
1 0 31	1.6419	1.6421	19
$\bar{1}$ 0 32	1.6068	1.6067	25
1 1 21	1.4538	1.4535	55

Schneider *et al.* in the temperature range of 1000 to 1500°C (*18*). They reported an X-phase which is similar to κ-alumina. MacDonald *et al.* (*20*) confirmed the X-phase which was obtained at 1580°C for a heating period of 16 hr. On the other hand, Shannon and Prewitt (*21*) studied the Ga_2O_3–In_2O_3 system both under normal and high pressures above 1000°C and reported that there was no binary compound but a solid solution of $In_xGa_{2-x}O_3$ ($x = 0 \sim 1$) with the β-Ga_2O_3 structure under a normal pressure. In the present work, we could not obtain any binary compounds but we did find a continuous series of solid solutions with the β-Ga_2O_3 structure ranging to $InGaO_3$, which is in good agreement with the result reported by Shannon and Prewitt. A solid solution range of In_2O_3 was considered to be negligibly narrow. In the In_2O_3–Ga_2O_3–CuO system, $InGaCuO_4$ and $In_2Ga_2CuO_7$ were found. It was concluded through X-ray powder diffraction data that (In $O_3)_n$CuO (n = 1 and 2) were isostructural with $(YbFeO_3)_n$FeO (n = 1 and 2). Their indexing, d-spacings, and relative intensities are listed in Table I and the lattice constants are shown in Table II. From the results above, we can conclude that the Cu^{2+} ion in $(InGaO_3)_n$CuO occupies the position of Fe^{2+} in $YbFe_2O_4$ and $Yb_2Fe_3O_7$ compounds, respectively.

We heated the $In_2Ga_2CuO_7$ at 1100°C for 1 week and no decomposition was detected. Both the mixtures of $In_2O_3 : Ga_2O_3 : CuO = 0.375 : 0.375 : 0.25$ and $In_2O_3 : Ga_2O_3 :$ CuO $= 0.40 : 0.40 : 0.20$ were

TABLE II

LATTICE CONSTANTS OF THE NEW COMPOUNDS AS A HEXAGONAL CRYSTAL SYSTEM

	$InFeCuO_4$	$InGaCuO_4$	$InGaCoO_4$	$In_2Ga_2CuO_7$
a (Å)	3.3743(4)	3.3497(2)	3.3091(2)	3.3319(1)
c (Å)	24.841(5)	24.822(3)	25.859(4)	28.697(2)

	$In_2Fe_2CuO_7$	$In_2FeGaCuO_7$	$In_3Fe_3CuO_{10}$
a (Å)	3.3515(2)	3.3421(2)	3.3432(3)
c (Å)	28.871(3)	28.817(3)	61.806(6)

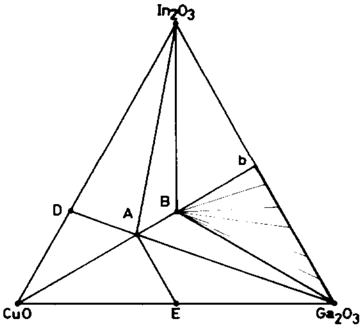

FIG. 4. The phase diagram of the In_2O_3–Ga_2O_3–CuO system at 1000°C. (A) $InGaCuO_4$, (B) $In_2Ga_2CuO_7$, (D) $In_2Cu_2O_5$, (E) Ga_2CuO_4, (b) $In_2O_3 : Ga_2O_3 = 1 : 1$ (in moles).

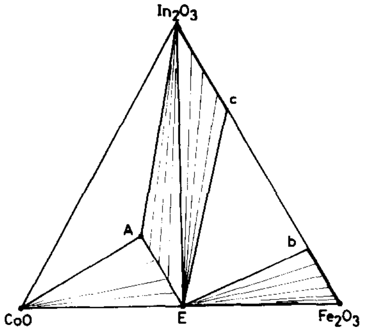

FIG. 5. The phase diagram of the In_2O_3–Fe_2O_3–CoO system at 1300°C. (A) $InFeCoO_4$ (spinel), (E) Fe_2CoO_4, (b) $In_2O_3 : Fe_2O_3$ = 0.25 : 0.75 (in moles). (c) $In_2O_3 : Fe_2O_3$ = 0.60 : 0.40 (in moles).

heated at 1100°C for 1 week; however, neither $In_3Ga_3CuO_{10}$ nor $In_4Ga_4CuO_{13}$ was observed. $(InGaO_3)_nCuO$ (n = 1 and 2) were heated at 700°C in air for 27 days and no decompositions of either phase was detected and the powder pattern of each compound became sharper as the heating period became longer. The phase relations of the In_2O_3–Ga_2O_3–CuO system at 1000°C is shown in Fig. 4. Substituting one of the Ga atoms in the $In_2Ga_2CuO_7$ by an Fe atom gave $In_2GaFeCuO_7$, having $Yb_2Fe_3O_7$ structure. Powder X-ray data and lattice constants for it are shown in Tables I and II, respectively.

[*III*] *The Phase Relations in the In_2O_3–Fe_2O_3–CoO System at* 1300°C

In the In_2O_3–CoO system, no binary compound was detected. The In_2CoO_4 phase with an inverse spinel structure (*22*) could not be detected as a stable compound. In the CoO–Fe_2O_3 system, there was a wide solid solution range of a spinel phase, "Fe_2CoO_4." Masse and Muan (*23*) carefully studied the Fe_3O_4–Fe_2O_3–CoO system at elevated temperatures in air and reported the range of the compositional change in the spinel phase. According to them, the spinel structure exists at 1300°C in compositions Fe_2O_3 : CoO = 0.88 : 0.12–0.44 : 0.56. The compositional range in the phase relations shown in Fig. 5 is taken from Masse and Muan. In the Fe_2O_3–In_2O_3 system, no binary compound was observed, and we concluded that the solid solution range of Fe_2O_3 attained to $In_2O_3 : Fe_2O_3$ = 0.25 : 0.75 and that of In_2O_3 attained to $In_2O_3 : Fe_2O_3$ = 0.60 : 0.40.

In the In_2O_3–Fe_2O_3–CoO system, there was a ternary compound, $InFeCoO_4$ with a spinel structure and a continuous series of spinel solid solutions between $InFeCoO_4$ and Fe_2CoO_4. The lattice constants of the solid solutions are shown in Fig. 6. These solid solutions follow Vegard's law as shown in the figure. The compositions were not determined analytically but were assumed to have the original composition since no second phases were detected. A spinel phase region in the In_2O_3–Fe_2O_3–CoO system is shown together with stable phases in Fig. 5.

[*IV*] *The Phase Relations in the In_2O_3–Ga_2O_3–CoO System at* 1300°C

In the CoO–Ga_2O_3 system, there was a Ga_2CoO_4 phase with a spinel structure. The solid solution range of the spinel was much narrower than that of Fe_2CoO_4 phase. In the Ga_2O_3–In_2O_3 system, no binary compound was detected, but a solid solution

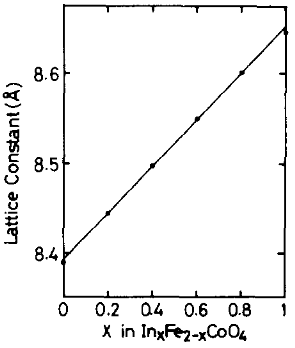

FIG. 6. Lattice constants of the spinel solid solutions $In_xFe_{2-x}CoO_4$.

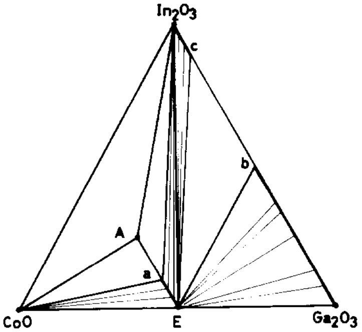

FIG. 7. The phase diagram of the In_2O_3–Ga_2O_3–CoO system at 1300°C. (A) $InGaCoO_4$ ($YbFe_2O_4$ type), (E) Ga_2CoO_4, (a) $In_2O_3 : Ga_2O_3 : CoO = 0.10 : 0.40 : 0.50$ (in moles). (b) $In_2O_3 : Ga_2O_3 = 1 : 1$ (in moles).

range of the β-Ga_2O_3 phase reached $InGaO_3$, which is in good agreement with the data reported by Shannon and Prewitt (*21*), and the In_2O_3 phase reached the composition $In_2O_3 : Ga_2O_3 = 0.90 : 0.10$. The X-phase which had been reported by Schneider *et al.* (*18*) was not detected even at 1300°C. In the In_2O_3–Ga_2O_3–CoO system, there was a stable ternary compound, $InGaCoO_4$ with the $YbFe_2O_4$ structure. Powder X-ray diffraction data are shown in Table I; lattice constants, in Table II. Rather extensive solubility of $InGaCoO_4$ in the spinel phase, Ga_2CoO_4 is observed. The solid solution ranges from Ga_2CoO_4 to $In_{0.4}Ga_{1.6}CoO_4$, and the lattice constant varies from $a = 8.3229(1)$ Å (Ga_2CoO_4) to $a = 8.4260(4)$ Å ($In_{0.4}Ga_{0.6}CoO_4$). The phase relations in the In_2O_3–Ga_2O_3–CoO system at 1300°C is shown in Fig. 7.

The experimental data which establish each of the phase relations in the In_2O_3–A_2O_3–BO systems at elevated temperatures are shown in Table III.

When $InGaCoO_4$ with the $YbFe_2O_4$ structure was heated at 1500°C for 10 days, it changed to a spinel type compound. It reversibly converted to a $YbFe_2O_4$ type compound at 1300°C. On the other hand, the $YbFe_2O_4$ type of $InGaCoO_4$ decomposed to

TABLE IIIa

THE PHASE RELATIONS IN THE In_2O_3–A_2O_3–CuO SYSTEM AT 1000°C

In_2O_3–Fe_2O_3–CuO			In_2O_3–Ga_2O_3–CuO		
Composition (mole ratio)	Period (days)	Phases	Composition (mole ratio)	Period (days)	Phases
1 : 0 : 2	10	2–2–5	0 : 1 : 1	6	Ga_2CuO_4
1 : 1 : 2	10	1–1–1–4	1 : 0 : 2	7	$In_2Cu_2O_5$
1 : 1 : 1	10	2–2–1–7	1 : 1 : 2	14	1–1–1–4
3 : 3 : 2	10	3–3–1–10	1 : 1 : 1	14	2–2–1–7
1 : 8 : 1	27	2–2–1–7, Fe_2CuO_4, Fe_2O_3	25 : 35 : 40	24	1–1–1–4, 2–2–1–7, Ga_2O_3
15 : 75 : 10	27	2–2–1–7, 3–3–1–10, Fe_2O_3	40 : 25 : 30	10	1–1–1–4, 2–2–1–7, In_2O_3
20 : 75 : 5	24	3–3–1–10, Fe_2O_3, In_2O_3	75 : 75 : 50	24	2–2–1–7, Ga_2O_3
20 : 70 : 10	24	3–3–1–10, In_2O_3, Fe_2O_3	15 : 5 : 80	12	CuO, $In_2Cu_2O_5$, 1–1–1–4
70 : 20 : 10	24	3–3–1–10, In_2O_3	40 : 10 : 50	12	$In_2Cu_2O_5$, 1–1–1–4, In_2O_3
20 : 55 : 25	32	2–2–1–7, Fe_2CuO_4, Fe_2O_3	5 : 65 : 30	26	Ga_2O_3, Ga_2CuO_4, 1–1–1–4
25 : 35 : 40	20	2–2–1–7, 1–1–1–4, Fe_2CuO_4	10 : 20 : 70	12	1–1–1–4, CuO, Ga_2CuO_4
40 : 25 : 35	6	In_2O_3, 1–1–1–4, 2–2–1–7	95 : 95 : 10	113	2–2–1–7, Ga_2O_3
40 : 10 : 50	10	In_2O_3, 1–1–1–4, $In_2Cu_2O_5$	15 : 60 : 25	36	1–1–1–4, Ga_2O_3, 2–2–1–7
15 : 5 : 80	18	1–1–1–4, CuO, $In_2Cu_2O_5$	20 : 75 : 5	36	2–2–1–7, Ga_2O_3
5 : 65 : 30	18	2–2–1–7, Fe_2O_3, Fe_2CuO_4	1 : 1 : 0	111	Ga_2O_3
1 : 1 : 0	180	In_2O_3, Fe_2O_3	35 : 60 : 5	36	2–2–1–7, Ga_2O_3
95 : 95 : 10	60	3–3–1–10, In_2O_3, Fe_2O_3			
1 : 2 : 7	10	1–1–1–4, CuO, Fe_2CuO_4			1–1–1–4: $InGaCuO_4$
45 : 30 : 25	15	3–3–1–10, 2–2–1–7, In_2O_3			2–2–1–7: $In_2Ga_2CuO_7$
		2–2–5: $In_2Cu_2O_5$			
		1–1–1–4: $InFeCuO_4$			
		2–2–1–7: $In_2Fe_2CuO_7$			
		3–3–1–10: $In_3Fe_3CuO_{10}$			

TABLE IIIb

THE PHASE RELATIONS IN THE In_2O_3–A_2O_3–CoO SYSTEM AT 1300°C

In_2O_3–Fe_2O_3–CoO			In_2O_3–Ga_2O_3–CoO		
Composition (mole ratio)	Period (days)	Phases	Composition (mole ratio)	Period (days)	Phases
0 : 1 : 1	6	Spinel	0 : 1 : 1	6	Spinel
1 : 1 : 2	4	Spinel	1 : 1 : 2	6	$InGaCoO_4$
15 : 35 : 55	6	Spinel	1 : 4 : 5	6	Spinel
20 : 30 : 50	6	Spinel	5 : 1 : 4	6	In_2O_3, $InGaCoO_4$, CoO
10 : 40 : 50	6	Spinel	2 : 1 : 7	10	In_2O_3, $InGaCoO_4$, CoO
5 : 45 : 50	6	Spinel	1 : 6 : 3	6	Spinel, Ga_2O_3
40 : 25 : 35	6	Spinel, In_2O_3	1 : 8 : 1	8	Spinel, Ga_2O_3
60 : 30 : 10	6	In_2O_3, spinel	1 : 2 : 7	8	$InGaCoO_4$, CoO, spinel
30 : 55 : 15	6	In_2O_3, Fe_2O_3, spinel	1 : 1 : 1	8	In_2O_3, spinel
1 : 1 : 1	6	In_2O_3, spinel	5 : 2 : 3	10	In_2O_3, $InGaCoO_4$, spinel
4 : 1 : 5	13	In_2O_3, spinel, CoO	2 : 7 : 1	10	Spinel, Ga_2O_3
1 : 2 : 7	13	Spinel, CoO	50 : 35 : 15	10	In_2O_3, spinel, Ga_2O_3
10 : 55 : 35	13	Spinel, In_2O_3, Fe_2O_3	7 : 3 : 0	13	In_2O_3
1 : 0 : 2	13	In_2O_3, CoO	1 : 1 : 0	19	Ga_2O_3
25 : 50 : 25	7	In_2O_3, spinel, Fe_2O_3	1 : 2 : 0	19	Ga_2O_3
5 : 70 : 25	7	Spinel, Fe_2O_3			
50 : 35 : 15	16	Spinel, In_2O_3			
1 : 1 : 0	35	In_2O_3, Fe_2O_3			

In_2O_3, a spinel phase, and CoO after heat treatment at 1100°C for 3 days. The $InFeCoO_4$ having a spinel structure also decomposed to In_2O_3, a spinel phase, and CoO after heat treatment at 1100°C for 3 days. In the $LnABO_4$ (*Ln:* lanthanoid elements and Y, *A:* trivalent metal, *B:* divalent metal) isostructural with $YbFe_2O_4$, the transition to spinel structure has never been observed (*11*), while it is possible in $InGaCoO_4$. This may be due to the rather small ionic radius of In^{3+} compared with that of the lanthanide elements. Detailed study on this transition is in progress.

It is interesting to note the difference between Fe^{3+} and Ga^{3+} from the structural point of view. It is well known that Ga^{3+} has a slightly smaller ionic radius than Fe^{3+} and prefers a tetrahedral site to an octahedral one under a normal pressure (*24*). However, in the In_2O_3–A_2O_3–CuO systems, Fe^{3+} and Ga^{3+} seem to play similar roles in view of the formation of layered structures. $(InFeO_3)_nCuO$ ($n = 1$, 2, and 3) were found in the In_2O_3–Fe_2O_3–CuO system as well as $(InGaO_3)_nCuO$ ($n = 1$ and 2) in the In_2O_3–Ga_2O_3–CuO system. In contrast, $InFeCoO_4$ never takes the $YbFe_2O_4$ structure but a spinel one, while the $InGaCoO_4$ takes the layered structure at 1300°C. Considering the large ionic radius of In^{3+}, it was postulated that the $InFeCoO_4$ takes a structure denoted as Fe[InCo]O_4 which is formed simple replacement of Fe^{3+} by In^{3+} in an inverse spinel, Fe[FeCo]O_4 (*26*). Similarly, it can be expected from tetrahedral site preferency of Ga^{3+} that spinel type of $InGaCoO_4$ takes a structure, Ga[InCo]O_4. Table IV shows the possible sites and ionic radii of the cations after Shannon and Prewitt (*25*), when $InGaCoO_4$ and $InFeCoO_4$ take both spinel and $YbFe_2O_4$ structure (though $InFeCoO_4$ does not, really, take the $YbFe_2O_4$ structure). As shown in this table, the difference between ionic radii of five-coordinated Fe^{3+} and Ga^{3+} is very small, as well as between four-coordinated ones. Based upon the simple spherical ionic

TABLE IV

THE IONIC RADII (Å) AND COORDINATION NUMBERS OF In^{3+}, Co^{2+}, Fe^{3+}, AND Ga^{3+} WHEN THE $InFeCoO_4$ OR THE $InGaCoO_4$ HAS THE SPINEL OR THE $YbFe_2O_4$ STRUCTURE ACCORDING TO REF. (*25*)

Compound	$InFeCoO_4$	$InGaCoO_4$
Spinel type	In^{3+}(VI):0.80 Co^{2+}(VI):0.745 Fe^{3+}(IV):049	In^{3+}(VI):0.80 Co^{2+}(VI):0.745 Ga^{3+}(IV):0.47
$YbFe_2O_4$ type	In^{3+}(VI):0.80 Co^{2+}(V):0.67 Fe^{3+}(V):0.58	In^{3+}(VI):0.80 Co^{2+}(V):0.67 Ga^{3+}(V):0.55

O^{2-}:1.40
Fe^{3+} and Co^{2+}: high spin state

model, we cannot, therefore, explain the reason why $InFeCoO_4$ prefers the spinel structure. It is, however, shown through the present work that the $YbFe_2O_4$ structure is not, thermochemically, widely different from the spinel type, but in the case of $InACoO_4$, the factors controlling the type of the structure may be very critical.

In view of the discrepancy between the present work and that of Schneider *et al.* (*18*) for the In_2O_3–Ga_2O_3 system at elevated temperatures, further investigations of the system are desirable, especially the X-phase.

References

1. (i) N. Kimizuka and T. Katsura, *Bull. Chem. Soc. Jpn.* **47,** 1801 (1974), (ii) N. Kimizuka, A. Yamamoto, H. Ohashi, T. Sugihara, and T. Sekine, *J. Solid State Chem.* **49,** 65 (1983).

2. K. Kato, I. Kawada, N. Kimizuka, and T. Katsura, *Z. Kristallogr.* **141,** 314 (1975).

3. K. Kato, I. Kawada, N. Kimizuka, I. Shindo, and T. Katsura, *Z. Kristallogr.* **143,** 278 (1976).

4. Y. Matsui, K. Kato, N. Kimizuka, and S. Horiuchi, *Acta Crystallogr. Sect. B* **35,** 561 (1976).

5. N. Kimizuka, K. Kato, I. Kawada, I. Shindo, and T. Katsura, *Acta Crystallogr. Sect. B* **32,** 1721 (1976).

6. M. Tanaka, J. Akimitsu, Y. Inada, N. Kimizuka, I. Shindo, and K. Siratori, *Solid State Commun.* **44,** 687 (1982).

7. (i) Y. Nakagawa, M. Inazumi, N. Kimizuka, and K. Siratori, *J. Phys. Soc. Jpn.* **47,** 1669 (1979). (ii) M. Inazumi, Y. Nakagawa, M. Tanaka, N. Kimizuka, and K. Siratori, *J. Phys. Soc. Jpn.* **50,** 538 (1981).

8. E. J. Verway and P. W. Haayman, *Physica* **8,** 979 (1941).

9. C. Schlenker and M. Marezio, *Philos. Mag.* [*Part*] *B* **42,** 453 (1980).

10. (i) N. Kimizuka and E. Takayama, *J. Solid State Chem.* **42,** 22 (1982), (ii) N. Kimizuka and E. Takayama, *J. Solid State Chem.* **43,** 278 (1982).

11. (i) N. Kimizuka and E. Takayama, *J. Solid State Chem.* **40,** 109 (1981), (ii) N. Kimizuka and E. Takayama, *J. Solid State Chem.* **41,** 166 (1982).

12. M. Tanaka, N. Kimizuka, J. Akimitsu, S. Funahashi, and K. Siratori, *J. Magn. Magn. Mater.* **31/34,** 769 (1983).

13. J. H. W. De Wit, *J. Solid State Chem.* **13,** 192 (1975).

14. ASTM 13-534, Joint Committee of Powder Diffraction Data.

15. Yu. D. Tretyacov, V. F. Komorov, N. A. Prosvirnina, and I. B. Kusenok, *J. Solid State Chem.* **5,** 157 (1972); Yu. D. Tretyacov, A. R. Kaul, and N. V. Makuhin, *J. Solid State Chem.* **17,** 183 (1976).

16. G. Bergrhoff and H. Kasper, *Acta Crystallogr. Sect. B* **24,** 388 (1968).

17. A. M. M. Gadalla and J. White, *Trans. Brit. Ceram. Soc.* **63,** 1 (1964); D. S. Burst, A. M. M. Gadalla and J. White, *Trans. Brit. Ceram. Soc.* **64,** 731 (1965).

18. S. J. Schneider, R. S. Roth, and J. L. Waring, *J. Res. Nat. Bur. Stand. A* **65,** 345 (1961).

19. S. Geller, *J. Chem. Phys.* **33,** 676 (1960).

20. J. MacDonald, J. A. Card, and F. P. Glasser, *J. Inorg. Nucl. Chem.* **29,** 661 (1967).

21. R. D. Shannon and C. T. Prewitt, *J. Inorg. Nucl. Chem.* **30,** 1389 (1968).

22. R. C. Evans, "Introduction to Crystal Chemistry" 2nd. ed., p. 173, Univ. Press, Cambridge (1966).

23. D. P. Masse and A. Muan, *J. Amer. Ceram. Soc.* **48,** 466 (1965).

24. S. Geller, *Z. Kristallogr.* **125,** S. 1 (1967).

25. R. D. Shannon and C. T. Prewitt, *Acta Crystallogr. Sect. B* **25,** 925 (1969); R. D. Shannon and C. T. Prewitt, *Acta Crystallogr. Sect. B* **26,** 1046 (1970).

26. R. W. G. Wyckoff, "Crystal Structure Data," Chap. VIII, Part B, 2nd. ed., Vol. 3, Interscience, New York/London/Sydney (1960).